Nanocomposite Contact Material for MEMS Switches

C. Ding, N.C. MacDonald

Room 2229, ESB, University of California
Santa Barbara, CA, USA, ding@engr.ucsb.edu

ABSTRACT

This work introduces the fabrication and characterization of titania composite material by sputtering metals into nanostructured titania (NST) forming nanocomposite contact material. This nanostructured composite contact material is developed for improving the contact reliability of MEMS switches. The nanocomposite material is integrated into a bulk titanium MEMS (BT-MEMS) switch which is fabricated using a sacrificial layer free (SLF) processing technique. Above 15 billion cold contact cycles is achieved without adhesion failure.

Keywords: MEMS switch, nanocomposite, titania, contact material, reliability.

1 INTRODUCTION

MEMS switches are insensitive to acceleration and have advantages such as ultra low power consumption (for electrostatic actuation), very high cut-off frequency and linearity. Also due to outstanding isolation and low insertion loss performance at microwave frequencies, they can replace the GaAs switches in cellular telephones resulting in much lower DC-Power consumption and longer battery life. They can also be used in phase shifters in radar systems, in low loss tunable circuits for network matching, and in high-performance instrumentation systems. More detailed applications and lifetime requirements for each application are well summarized in Rebeiz's book [1]. To date, according to contact styles, two main types of switches have been developed: metal-to-metal contact switches[2-7], and capacitive contact[8, 9] switches. Gold is found to be a common contact material used for metal contact types.

Hard materials with good conductivity and rough surfaces are preferred for MEMS contact switches[10-14]. A hard contact material can help reduce the adhesion force by maintaining the required surface roughness, plastic deformation and creep of the material. Pure gold as a contact material is considered to be the best corrosion resistance among metals[15]. However it is very soft[10] and it easily creeps[11] under contact, leading to a polishing effect of the contact surfaces and a higher adhesion force between contacts. For MEMS switches this increase in adhesion force causes stiction between contacts and failure of the device. The straight forward solution to this stiction problem is to reduce the adhesion force by increasing either the material hardness[16] or surface roughness[13, 17-19]. The nanostructured Titania (NST) composite material offers potential to achieve both the above mentioned surface properties.

This paper will show a novel method to combine the NST with sputtered metals to form NST-Metal composite contact material (Fig. 1). With this material we achieved a high roughness (~30nm) and hardness (~3GPa) of the contact surfaces which were measured using AFM and nanoindenter respectively. Finally this paper shows how to integrate this new composite contact material into BT-MEMS switches for reliability test. Contact contamination was investigated using Auger system, and contamination mechanism is discussed.

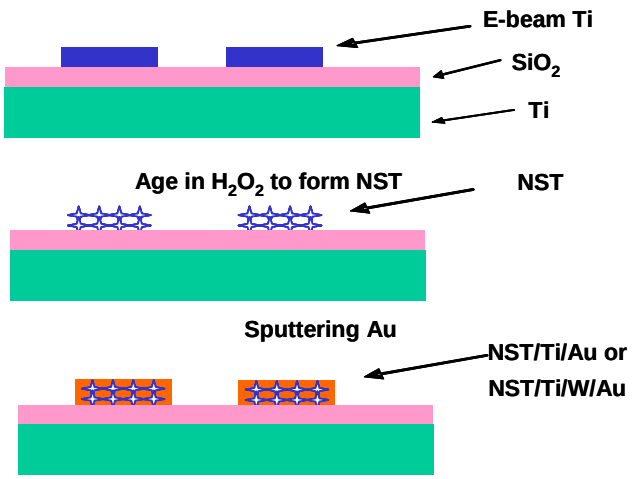

Figure 1: The NST was fabricated on a 400μm thick Ti substrate. After annealing, 0.5μm thick E-beam evaporated Ti was deposited on the top with lift-off technique.

2 NANOCOMPOSITE CONTACT MATERIAL

This novel nanocomposite contact material is based on filling nano-structured titania (NST) with metals. The NST is formed by oxidizing e-beam evaporated titanium thin film in diluted hydrogen peroxide solution. The was introduced in the work of Aimi[20]. Simple experiments

were done by depositing Au directly onto NST leading to the result of delamination of the Au film from the NST layer. To solve the delamination problem, the metals need to grow on the wires or walls of the pores and then expand outwards to seal the pores.

The NST/Au composite material produces good surface properties as a contact material for MEMS switches. Figure 1 illustrates the fabrication of the NST composite fabrication. A 1μm thick silicon dioxide layer was first deposited onto the Ti substrate for electrical isolation. Then the E-beam deposited Ti was evaporated onto the SiO_2 layer. The E-beam Ti layer is 0.5μm thick, and it was evaporated onto SiO2 layer using a lift-off technique. The lift-off process flow is a simplified process which avoids etching for patterning the Ti film. The NST was aged in 10% H_2O_2 solution for 6 minutes at 83 ± 2^0C. Before deposition of other metals NST was annealed in oven at 350^0C for 10 hours.

2.1 Forming NST/Au nanocomposite

We show in this subsection the process to form NST-Metal composite by growing titanium, tungsten and gold on NST using sputtering technique. Figure 2 shows the SEM photographs of the above process description starting from NST to NST-Metal composite. Since gold does not adhere to NST, delamination was observed after deposition of gold on NST. A thin layer of titanium is used as an adhesion layer between gold and NST. Also a tungsten layer was found to be a good diffusion barrier layer to avoid titanium oxide formation on the gold surface (as mentioned in Fig.1).

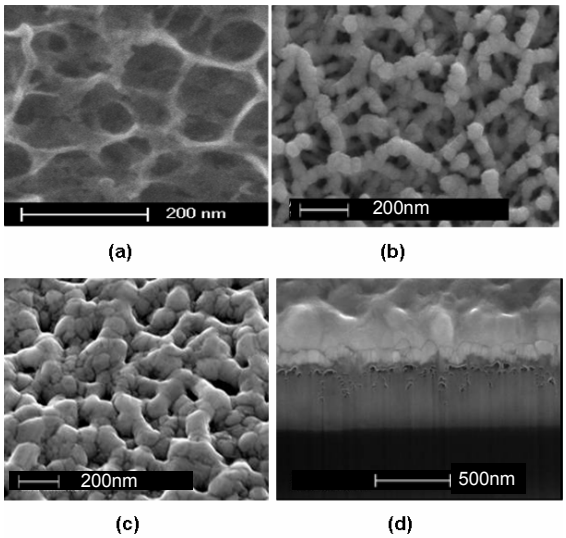

Figure 2: Fabrication of the nanocomposite material. (a) NST with pore size around 200nm in diameter; (b)NST/Ti10nm/W40nm, use titanium as adhesion layer, and use tungsten as diffusion barrier layer; (c)NST/Ti10nm/W40nm/Au100nm; (d)Cross section of NST/Ti10nm/W40nm/Au250nm.

The surface hardness of this NST/Au composite was characterized with a TriboIndenter made by Hysitron Inc. The TriboIndenter is a stand-alone nanomechanical testing system, which is designed to provide fully automated testing and in-situ imaging of the material. During the test a 2D transducer is used to provide an indentation force as high as 1mN. A load is applied starting from 50μN to 1000 μN with an increase of 50μN/step. A cubic corner tip with a tip radius of 40nm was used for hardness test. Due to the inter-network structure of the NST composite material surface, the hardness on the surface is simply not uniform. The bumps which are more solid and strengthened by NST/Au composite are harder than the valley areas where there may be voids underneath; this contributes to the non-uniformity of the NST-metal composite material. The elastic modulus for NST composite is around 128.35GPa, and the standard deviation value is 35GPa. The pure gold sample has the elastic modulus of 131.4GPa with a standard deviation of 12.67Gpa, which is quite consistent with the literature[21]. The hardness value at the top 100nm is about 3.7 GPa.

AFM (Atomic Force Microscope) is used to profile the surface of the original titanium thin film and the NST/Au composite material. The AFM data allows us to quantitatively analyze the surface roughness. An area of 2μmX2μm was scanned for imaging and roughness data collection. The surface roughness (RMS value) of NST/Au is ~31.03nm which is about two times higher than the original surface roughness (~10.6nm) of the deposited Ti thin film.

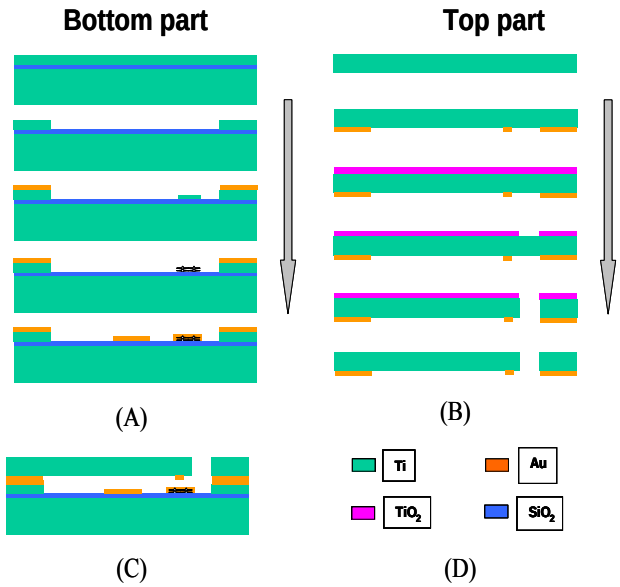

Figure 3: The processing flow for integrating the NST/Au nanocomposite with a bulk-titanium MEMS switch. (A) process flow for bottom part, (B) process flow for the top part, (C) bonding of the top and bottom parts using flip-chip bonder, (D) legends used.

NSTI-Nanotech 2009, www.nsti.org, ISBN 978-1-4398-1782-7 Vol. 1, 2009

2.2 Integration of the nanocomposite

The fabrication of a Bulk-Ti MEMS switch starts from a titanium-on-insulator (TOI) structure (similar to SOI substrate) was shown in Fig. 3a. The top layer (Fig. 3b) of titanium was sputter deposited. The top titanium film is around 2μm thick, and is patterned by a lift-off process or by dry etching for forming the gap between the electrodes (Fig 3c). The contact areas are oxidized by dipping the whole sample into the hydrogen peroxide.

Some patterned Ti areas used for bonding pads are not oxidized and these areas must be properly protected during oxidization. The process flow (Fig. 3) explains how the top and bottom parts are prepared to assemble the switch (Fig. 4).

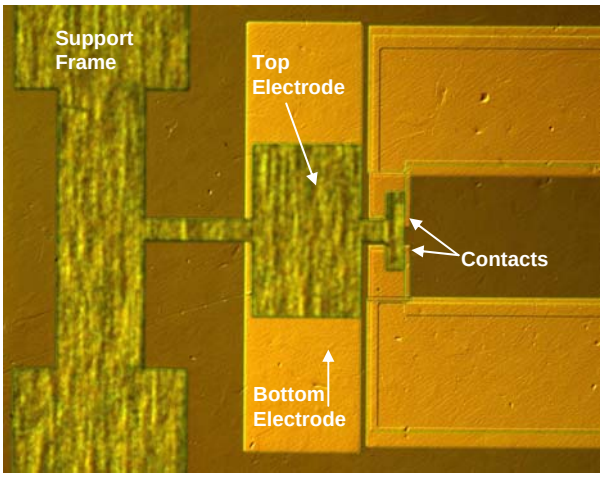

Figure 4: Microscope photograph view of the fabricated bulk titanium MEMS switches. The NST-Metal composite material was integrated into the bottom part of the switch. The two parts were assembled together using flip-chip bonding technique.

3 TESTING

The contact resistance was monitored during contacts with four point probe method. Figure 5 shows the measurable contact resistance plot according to the contact cycles. The contact resistance across the two contacts starts around 0.5Ohm and then slowly increased to 1Ohm at after about half million contact cycles, and finally goes up very sharply to 40.5 Ohm at around 1 million contact cycles. After this contact resistance values goes to a value that could not be monitored anymore.

The device was kept running at 10kHz for cold contact reliability test. No current was applied anymore for this test. We achieved above 15 billion cold contact cycles without adhesion failure. The contamination at the contact spot after 15 billion cold contact cycles was investigated using Auger system.

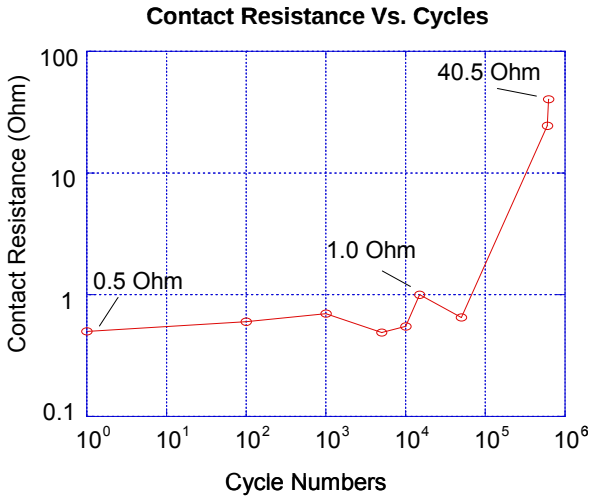

Figure 5: Contact resistance trends according to the contact cycle number. Note that the contact resistance is low (~0.5Ohm) starting from the beginning cycles. The low contact resistance at the beginning cycles benefits from the flip-chip bonding technique which eliminated the use of sacrificial layer and the contaminations caused by it.

4 ANALYSIS AND DISCUSSION

The contact resistance plot of the device shows a very low value (0.5Ohm) from the very beginning cycles. This preferred result of low contact resistance at the beginning cycles benefits from the asperities of the surfaces. The flip-chip bonding technique eliminated the use of sacrificial layer and its corresponding contaminations[22]. Hermetic packaging of this device is essential for contact resistance stability. With hermetic packaging, this nanocomposite contact material combining with the bulk-Ti MEMS switch offers a solid solution for solving MEMS switch reliability issues.

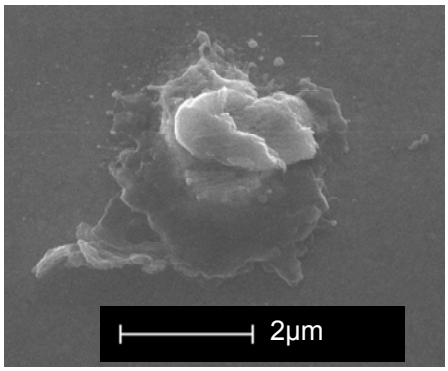

Figure 5: SEM of one contact spot on the bottom after 15 billion contact cycles.

The Auger analysis at the center of the contact spot (Fig.5) shows that the contamination at the contact spot mainly contains carbon (Fig. 6). We believe that the carbon contamination [3] was from the pump oil which originated from a mechanical pump that was used to vacuum the testing chamber.

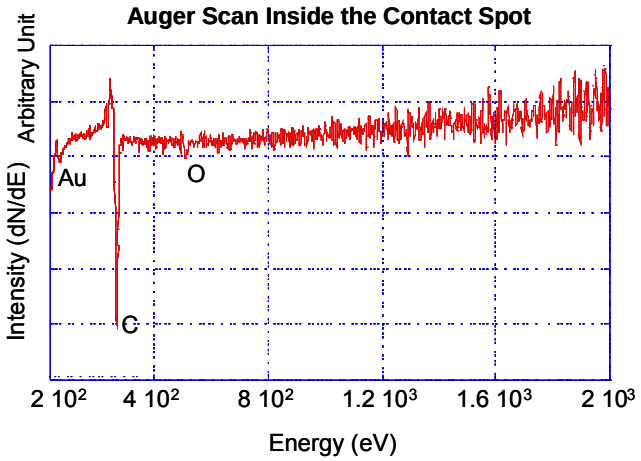

Figure 6: Auger scan at the contact spot shows that the carbon concentration is very high after 15 billion contact cycles. Very little gold was seen comparing to carbon.

5 CONCLUSION

Aqueous methods for fabrication of nanostructured titania were investigated. SEM studies show that the pores are in the range of 200nm, and that the sputtered metals grow on the wires and/or walls on the pores. AFM characterization of the surface showed that the roughness was increased two times larger then the original blank Ti films. The hardness at the nanocomposite surfaces are measured using nanoindentation techniques, its value is around 3.7GPa on the bumps and less harder on the valleys. Processes were developed for integrating NST composite material into MEMS switches. The switch had an NST/Au composite on the bottom contact, and sputtered gold on the top contacts. The switch underwent more than 15 billion contact cycles without adhesion failure. A good contact resistance value (~0.5 Ohm) was achieved with this switch for about half million cycles. Hydrocarbon contamination is believed to be the reason for the increase in contact resistance.

This work is supported by the Microsystems Technology Office at the Defense Advanced Research Projects Agency. A portion of this work was done in the UCSB nanofabrication facility, part of the NSF funded NNIN network.

REFERENCE

[1] Rebeiz, G.M., RF MEMS: Theory, Design and technology. 2003: Wiley.
[2] Coutu, R.A., Jr., et al., Microswitches with sputtered Au, AuPd, Au-on-AuPt, and AuPtCu alloy electric contacts. Components and Packaging Technologies, IEEE Transactions on, 2006. **29**(2): p. 341-349.
[3] Gretillat, M.A., F. Gretillat, and N.F. de Rooij, Micromechanical relay with electrostatic actuation and metallic contacts. Journal of Micromechanics and Microengineering, 1999. **9**(4): p. 324-331.
[4] Guan-Leng, T. and G.M. Rebeiz, A DC-contact MEMS shunt switch. Microwave and Wireless Components Letters, IEEE, 2002. **12**(6): p. 212-214.
[5] Hyman, D. and M. Mehregany, Contact physics of gold microcontacts for MEMS switches. Components and Packaging Technologies, IEEE Transactions, 1999. **22**(3): p. 357-364.
[6] Jensen, B.D., et al. Asperity heating for repair of metal contact RF MEMS switches. 2004.
[7] Jr, R.A.C., et al., Selecting metal alloy electric contact materials for MEMS switches. Journal of Micromechanics and Microengineering, 2004(8): p. 1157-1164.
[8] Melle, S., et al., Failure predictive model of capacitive RF-MEMS. Microelectronics and Reliability, 2005. **45**(9-11): p. 1770-1775.
[9] Yao, Z.J., et al., Micromachined low-loss microwave switches. Microelectromechanical Systems, Journal of, 1999. **8**(2): p. 129-134.
[10] Sauer, H., Modern Relay Technology. 1986, Huethig.
[11] Gregori, G. and D.R. Clarke, Mechanical creep as a life-limiting factor of radio frequency microswitches. Applied Physics Letters, 2005. **87**(15): p. 154101-3.
[12] Jemaa, N.B., et al., Erosion and contact resistance performance of materials for sliding contacts under arcing. Components and Packaging Technologies, IEEE Transactions on, 2001. **24**(3): p. 353-357.
[13] Kim, H.C. and T.P. Russell, Contact of elastic solids with rough surfaces. Journal of Polymer Science Part B-Polymer Physics, 2001. **39**(16): p. 1848-1854.
[14] Komvopoulos, K., Surface engineering and microtribology for microelectromechanical systems. Wear, 1996. **200**(1-2): p. 305-327.
[15] Hasegawa, M., et al. An experimental study on operating characteristics of Ag, Pd and Cu contacts in argon atmosphere. 2003.
[16] Lee, H., et al., Characterization of metal and metal alloy films as contact materials in MEMS switches. Journal of Micromechanics and Microengineering, 2006. **16**(3): p. 557-563.
[17] Tonck, A., et al., Electrical and mechanical contact between rough gold surfaces in air. Journal of Physics: Condensed Matter, 1991(27): p. 5195-5201.
[18] Persson, B.N.J. and E. Tosatti, The effect of surface roughness on the adhesion of elastic solids. Journal of Chemical Physics, 2001. **115**(12): p. 5597-5610.
[19] Greenwood, J.A. and J.J. Wu, Surface Roughness and Contact: An Apology. Meccanica, 2001. **36**(6): p. 617-630.
[20] Aimi, M.F., et al., High-aspect-ratio bulk micromachining of titanium. Nature Materials, 2004. **3**(2): p. 103-105.
[21] L. Siller, L., et al., Gold film with gold nitride -A conductor but harder than gold. 2005, AIP. p. 221912.
[22] Pacheco, S.P., L.P.B. Katehi, and C.T.C. Nguyen. Design of low actuation voltage RF MEMS switch. in Microwave Symposium Digest., 2000 IEEE MTT-S International. 2000.